DOUBLE SCROLL VIA A TWO-TRANSISTOR CIRCUIT

by

T. Matsumoto, L. O. Chua and K. Tokumasu

Memorandum No. M86/1

6 January 1986

Cover Page

DOUBLE SCROLL VIA A TWO-TRANSISTOR CIRCUIT

by

T. Matsumoto, L. O. Chua and K. Tokumasu

Memorandum No. M86/1

6 January 1986

ELECTRONICS RESEARCH LABORATORY

College of Engineering
University of California, Berkeley
94720

DOUBLE SCROLL VIA A TWO-TRANSISTOR CIRCUIT*

T. Matsumoto†, L.O. Chua†† and K. Tokumasu†

Abstract The double scroll attractor has been experimentally observed from an extremely simple circuit using an op amp. The purpose of this brief note is to give an alternate realization of the circuit using only two transistors as the active elements.

*Research sponsored by the Office of Naval Research Contract N00014-70-C-0572 and National Science Foundation Grant ECS-8313278.

† Department of Electrical Engineering
Waseda University
Tokyo 160, Japan

†† Department of Electrical Engineering and
Computer Sciences
University of California,
Berkeley, CA 94720

I. INTRODUCTION

The double scroll is a chaotic attractor associated with an extremely simple circuit recently reported and analyzed extensively in [1]. This circuit is made of 4 <u>linear</u> <u>passive</u> elements (2 capacitors, 1 inductor and 1 resistor) and 1 <u>nonlinear</u> <u>active</u> 2-terminal resistor characterized by a 3-segment piecewise-linear v-i characteristic. Because of its piecewise-linear character, this nonlinear element can be easily and accurately realized using an op amp, as was done in [1].

The purpose of this brief paper is to show that we can trade the op amp by two bipolar transistors. This circuit is more appealing to some researchers outside of the circuit theory community who automatically associate an op amp circuit with an analog computer.

The circuit to be presented in this paper will show beyond the shadow of a doubt that it is an intrinsic physical system whose chaotic behavior arises from complicated interactions between the instantaneous electric energy stored in the capacitors and the instantaneous magnetic energy stored in the inductors, where both voltages and currents play a crucial role.[†]

[†] In an analog computer, the node voltages are identified with the analog variables and hence the currents in the circuit elements are irrelevant.

II. OBSERVATION OF THE DOUBLE SCROLL

The autonomous (no time-dependent sources) circuit of Fig. 1 contains two rather <u>typical</u> transistors and diodes, in addition to several passive elements.

The dynamics of this circuit is described by the state equations

$$\boxed{\begin{aligned} C_1 \frac{dv_{C_1}}{dt} &= v_{C_2} - v_{C_1} - g(v_{C_1}) \\ C_2 \frac{dv_{C_2}}{dt} &= v_{C_1} - v_{C_2} + i_L \\ L \frac{di_L}{dt} &= -v_{C_2} \end{aligned}} \tag{1.1}$$

where v_{C_1} , v_{C_2} and i_L are the voltage across C_1 , the voltage across C_2 and the current through L, respectively, and g(.) is the v-i characteristic of the sub-circuit N enclosed by the broken line box. Figure 2(a) shows the measured v-i characteristic $g(\cdot)$ of N. Figure 2(b) shows an enlargement of this characteristic near the origin which covers the dynamic range of interest in this paper, namely, $|v| \leq 10$V. Note that this characteristic is almost piecewise-linear with break points at $v = \pm 1$V.

This piecewise-linear characteristic is also derived in the Appendix via a standard electronic circuit analysis technique.

Figure 3 shows the double scroll observed with the following element values:

$$\begin{array}{ll} C_1 = 0.0053\ \mu F, & C_2 = 0.047\ \mu F, \\ L = 6.8\ mH, & R = 1.21\ k\Omega, \\ R_B = 56\ k\Omega, & R = 1\ k\Omega, \\ R = 3.3\ k\Omega, & R = 88\ k\Omega, \\ R = 39\ k\Omega, & V_{cc} = 29\ V \end{array} \tag{1.2}$$

These are the nominal values; the exact values could be within 10% of (1. 2) due to component tolerances.

Figure 4 shows the time waveforms of the three state variables measured from the above circuit. Note that the dynamic range of v_{C_1} in the double scroll attractor is limited by

$$|v_{C_1}(t)| < 10 \text{ V for all } t.$$

Therefore the "passive portions" of $g(\cdot)$, i.e., the region $|v| > 15$ V of Fig. 2(a), has nothing to do with the attractor.

III. NUMERICAL CONFIRMATION

The previous results can be easily confirmed by a digital computer. A reasonably accurate transistor model is given by the well-known Ebers-Moll equations [2]:

$$\begin{aligned} i_E &= -\frac{I_s}{\alpha_F}\left(e^{v_{BE}/V_T}-1\right) + I_s\left(e^{v_{BC}/V_T}-1\right) \\ i_C &= I_s\left(e^{v_{BE}/V_T}-1\right) - \frac{I_s}{\alpha_R}\left(e^{v_{BC}/V_T}-1\right) \end{aligned} \tag{3.1}$$

where the variables are defined in Fig. 5, I_s is the saturation current and V_T is the thermal voltage.

All the computations in this section are done with SPICE2 [3], using the following model parameter values:

$$I_s = 10^{-12}\text{A},\ \alpha_F = \frac{\beta_F}{1+\beta_F},\ \alpha_R = \frac{\beta_R}{1+\beta_R}, \tag{3.2}$$

$$\beta_F = 181.5,\ \beta_R = 1,\ V_T = \text{room temperature.}$$

Figure 6 shows the double scroll seen by SPICE simulation using the model parameter values given by (3. 2) and the following element values:

$$
\begin{aligned}
C_1 &= 0.00565\ \mu F, & C_2 &= 0.05\ \mu F, \\
L &= 6.8\ mH, & R &= 1.26\ k\Omega, \\
R_B &= 59\ k\Omega, & R_1 &= 1\ k\Omega, \\
R_2 &= 3.25\ k\Omega, & R_3 &= 90\ k\Omega, \\
R_4 &= 39\ k\Omega, & V_{CC} &= 29.4\ v.
\end{aligned} \tag{3.3}
$$

Note that each of the element values in (3.3) is within 5% of the corresponding nominal value in (1.2). Figure 7 gives the SPICE simulated time waveforms. The correspondence with the experimental data is excellent.

APPENDIX ANALYSIS OF N

We will derive the v-i characteristic of N in Fig. 1.

Consider the circuit of Fig. 8 which is a subcircuit of N in Fig. 1. This 2-transistor circuit belongs to a family of negative-resistance devices analyzed in [6]. Let us consider first, the case where $v \geq 0$. There are three modes of operations for this circuit.

Mode 1: Both Q_1 and Q_2 are in the forward active region [4].

Note that this circuit is symmetric. Therefore, if $v_1 = 0$, then Q_1 and Q_2 must be operating in the same mode in some small neighborhood of the operating point; namely, forward active, reversed active, cut-off, or saturation. It is easy to see that Q_1 and Q_2 can not operate in the reversed active negion, or in the cut-off region, or in the saturation region, simultaneously. Hence they are in the forward active region. In this mode, each of the transistors can be approximately modelled by the linear circuit of Fig. 9, where $V_D \approx 0.7$ V is the "on voltage" and the diamond denotes a current controlled current source with a small-signal gain $h_{fe} = \beta_F$ and i_B denotes the small-signal base current. Using this model, we can easily derive i_1 in terms of v_1 of Fig. 8:

$$i = \frac{1 + \frac{R_B}{R_1} - h_{fe}}{2\ R_B}\ v_1 \quad . \tag{A.1}$$

A crucial observation here is that

(i) if

$$\boxed{h_{fe} > 1 + \frac{R_B}{R_1}} \tag{A.2}$$

the v_1-i_1 characteristic is locally active [5], i.e., the slope is negative, whereas

(ii) if

$$h_{fe} \leq 1 + \frac{R_B}{R_1} \tag{A.3}$$

the v_1-i_1 characteristic is locally passive, i.e., the slope is non-negative.

Mode 2: Q_2 is in the forward active region while Q_1 is in the cut-off region.

As one increases the value of $v_1 > 0$, the voltage v_{CEQ_2} across the collector and the emitter of Q_2 keeps decreasing. Moreover, the voltage v_{BEQ_1} across the base and the emitter of Q_1 drops even lower than v_{CEQ_2} because of R_B. Therefore, Q_1 would eventually cut off when $v_{BEQ_1} \approx V_D \approx 0.7$ V, i.e., $i_{BEQ_1}=0$. One can, then obtain i_1 in terms of v_1 in this mode:

$$i_1 = \frac{1 + \frac{R_B}{R_1}}{R_1(1 + h_{fe}) + 2R_B} v_1 - \frac{h_{fe}-1}{R_1(1 + h_{fe}) + 2R_B}(V_{cc}-V_D) \tag{A.4}$$

The value of v_1 at which Q_1 cuts off is given by

$$v_1^* = \frac{2R_B(V_{cc}-V_D)}{R_1(1 + h_{fe}) + R_B} \quad . \tag{A.5}$$

Note that in this mode, the coefficient of v_1 is positive and hence the associated v_1-i_1 characteristic is locally passive.

Mode 3: Q_2 is in the saturation region while Q_1 is in the cut-off region.

As one increases the value of $v_1 > 0$ further, the voltage v_{CEQ_2} keeps decreasing and it would eventually becomes 0, i.e., it would start saturating. An approximate transistor circuit model in the saturation region is given by Fig. 10. One can, then, obtain,

$$i_1 = \frac{R_1 R_B}{R_1+R_B} v_1 - \frac{V_{cc}}{R_1} - \frac{V_D}{R_B} \quad . \tag{A.6}$$

The v_1-i_1 characteristic is, again, locally passive. The value of v_1 at which Q_2 saturates is given by

$$v_1^{\#} = \frac{2 R_B V_{cc} + (1 + h_{fe}) R_1 V_D}{(1 + h_{fe})R_1 + R_B} \quad . \tag{A.7}$$

Since the circuit is symmetric, a similar analysis can be carried out for $v_1 < 0$. The entire $v_1 - i_1$ characteristic then, would look like Fig. 11 when $h_{fe} > 1 + \frac{R_B}{R_1}$ (see (A.2)). With the present parameter values, (1.2) or (3.3), the values v_1^* of (A.5) and $v_1^{\#}$ of (A.7) are close to each other.

Observe that the <u>base resistor</u> R_B <u>plays a crucial role</u> to keep v_1^* and $v_1^{\#}$ at appropriate values. If $R_B = 0$ as in [6], then $v_1^{\#}$ would be <u>very small</u>, and one would have a very small locally active region which unables one to design appropriate $v_1 - i_1$ characteristic.

Next, let us look at the resistor-diode circuit of Fig. 12 which is the remaining subcircuit of N. It is easy to see that the $v_2 - i_2$ characteristic would look like Fig. 12.

Since N consists of the parallel connection of the two subcircuits in Fig. 8 and Fig. 12, the composite v-i characteristic of N is obtained by superimposing Fig. 11 onto Fig. 13 and adding the ordinates to obtain Fig. 14, provided, of course, that appropriate element values are chosen. By substituting the actual element values in (1 . 2), we obtain a piecewise-linear characteristic which agrees remarkably well with that of Fig. 2.

REFERENCES

1. T. Matsumoto, L.O. Chua and M. Komuro, "The Double Scroll", IEEE Trans. CAS, vol. CAS-32, No.8, pp 797-818, 1985.
2. I.E. Getreu, Modelling the Bipolar Transistor, Elsevier Scientific Publishing Co., 1978.
3. A. Vladimirescu, K. Zhang, A.R. Newton, D.O. Pederson and A. Sangiovanni-Vincentelli, "SPICE version 2G User's Guide", Electronics Research Laboratory, University of California, Berkeley, Aug. 10, 1981.
4. V.H. Grinich and H.G. Jackson, Introduction to Integrated Circuits, McGraw-Hill, 1975.
5. L.O. Chua, "Dynamic Nonlinear Networks: State of the Art", IEEE Trans. CAS, vol. CAS-27, No. 11, pp 1059-1087, 1980.
6. L.O. Chua and A.C. Deng, "Negative Resistance Devices: Part II", Int. J. Circuit Theory and Applications, vol. 12, pp 337-373, 1984.

AKNOWLEDGEMENT We would like to thank T. Suzuki of Hitachi for discussions.

Figure Captions

Fig. 1 A 2-transistor circuit in which the double scroll is observed. Q_1, Q_2 = 2SC1815, D_1, D_2 = 1S1588.

Fig. 2 v-i characteristic of the broken line box.

(a) Global v-i characteristic. Horizontal axis: 5 V/division. Vertical axis : 5 mA/division.

(b) Blown up version. Horizontal axis: 1 V/division. Vertical axis: 1 mA/division.

Fig. 3 Measured double scroll.

(a) Projection onto the (i_L, v_{C_1})-plane. Horizontal axis: 2 mA/division. Vertical axis: 2 V/division.

(b) Projection onto the (i_L, v_{C_2})-plane. Horizontal axis: 2 mA/division. Vertical axis: 2 V/division.

(c) Projection onto the (v_{C_2}, v_{C_1})-plane. Horizontal axis: 2 V/division. Vertical axis: 2 V/division.

Fig. 4 Measured time waveforms of the three state variables.

(a) $v_{C_1}(t)$. Horizontal axis: 1 mS/division. Vertical axis: 2 V/division.

(b) $v_{C_2}(t)$. Horizontal axis: 1 mS/division. Vertical axis: 2 V/division.

(c) $i_L(t)$. Horizontal axis: 1 mS/division Vertical axis: 2 mA/division

Fig. 5 Symbol and variables associated with an npn transistor.

Fig. 6 Numerical confirmation of the observed double scroll.

(a) Projection onto the (i_L, v_{C_1})-plane.

(b) Projection onto the (i_L, v_{C_2})-plane.

(c) Projection onto the (v_{C_2}, v_{C_1})-plane.

Fig. 7 Simulated time waveforms.

(a) $v_{C_1}(t)$ (b) $v_{C_2}(t)$ (c) $i_L(t)$

Fig. 8 A subcircuit of N.

Fig. 9 Small-signal model of the transistor in the forward active region.

Fig. 10 Small-signal model of the transistor in the saturation region.

Fig. 11 The v_1-i_1 characteristic of N_1 in Fig. 8.

Fig. 12 Remaining subcircuit N_2 of N.

Fig. 13 The v_2 -i_2 characteristic of N_2 in Fig. 12.

Fig. 14 The composite v-i characteristic of N.

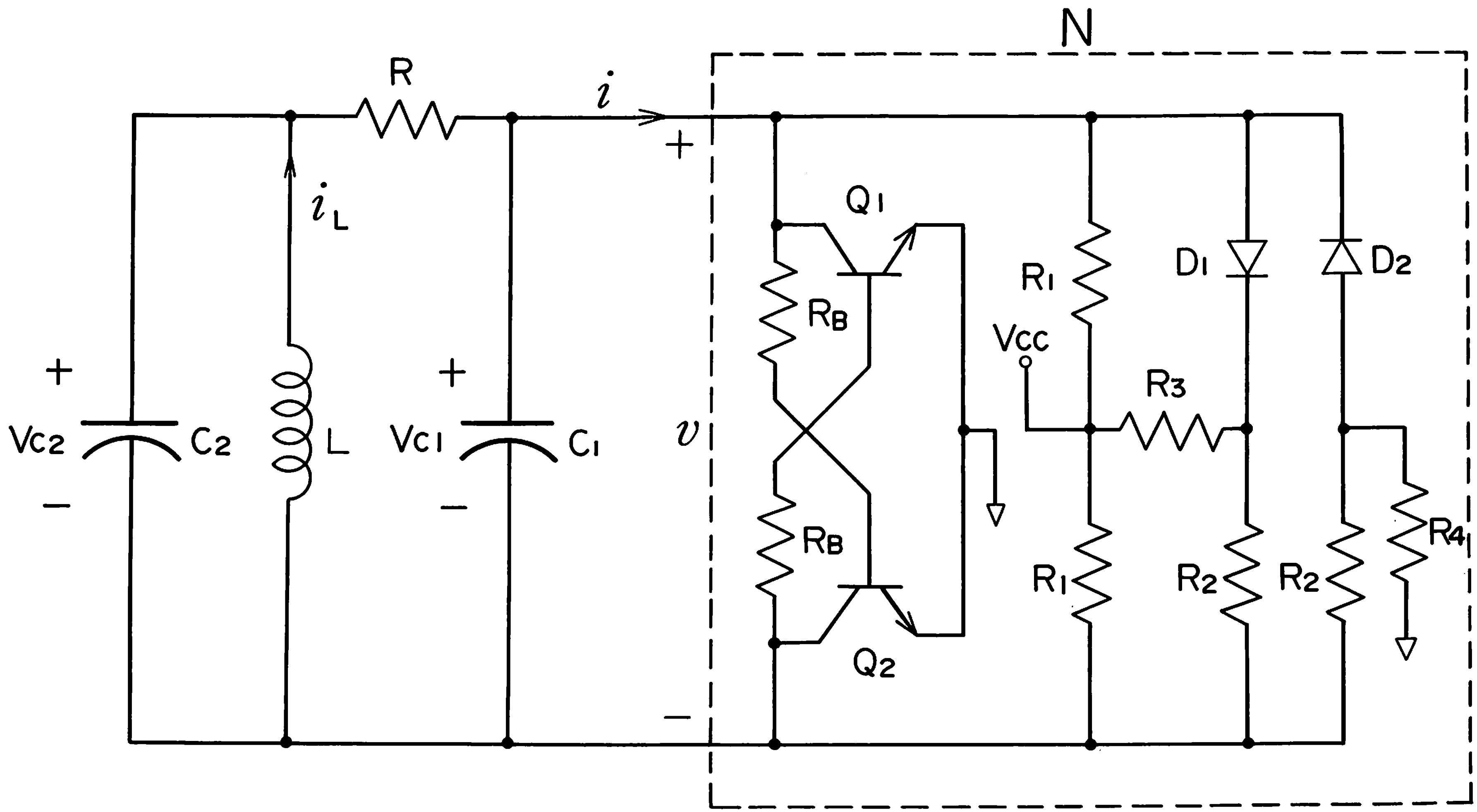

Fig.1

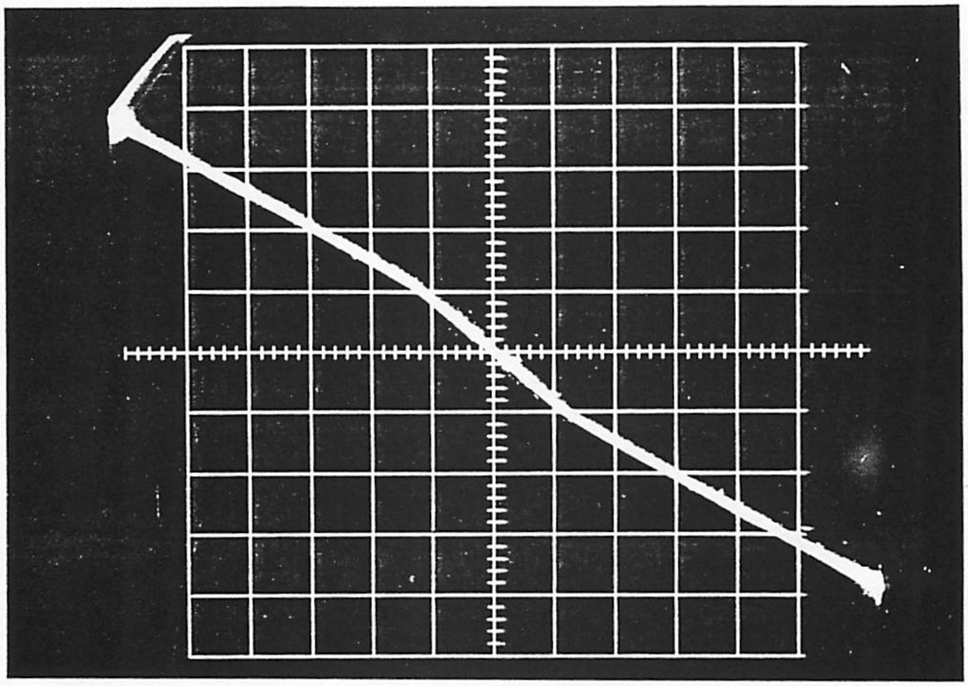

(a)

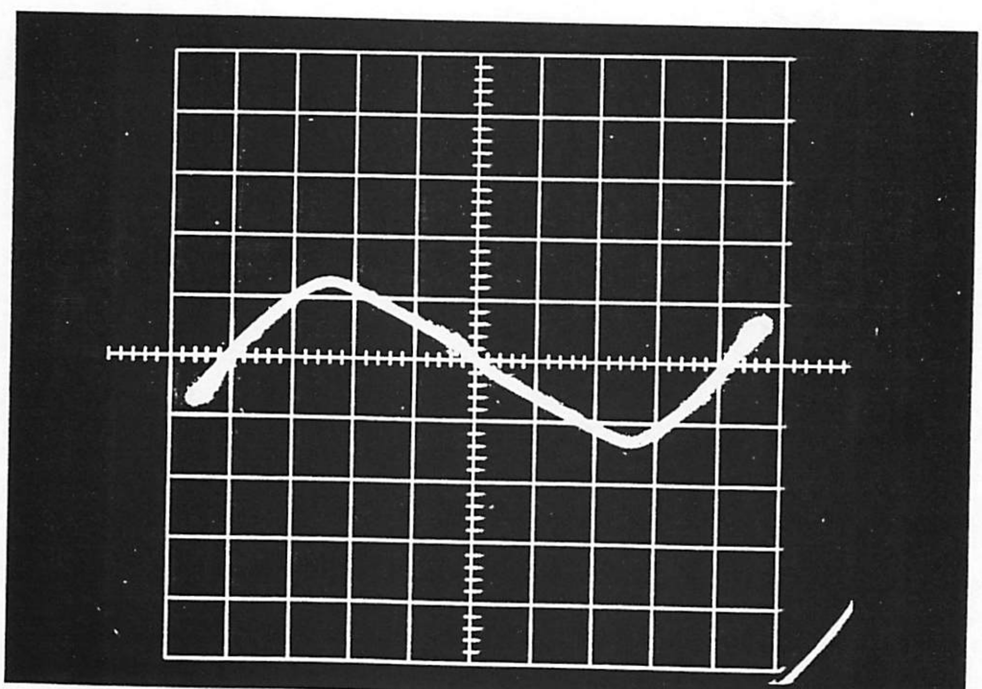

(b)

Fig. 2

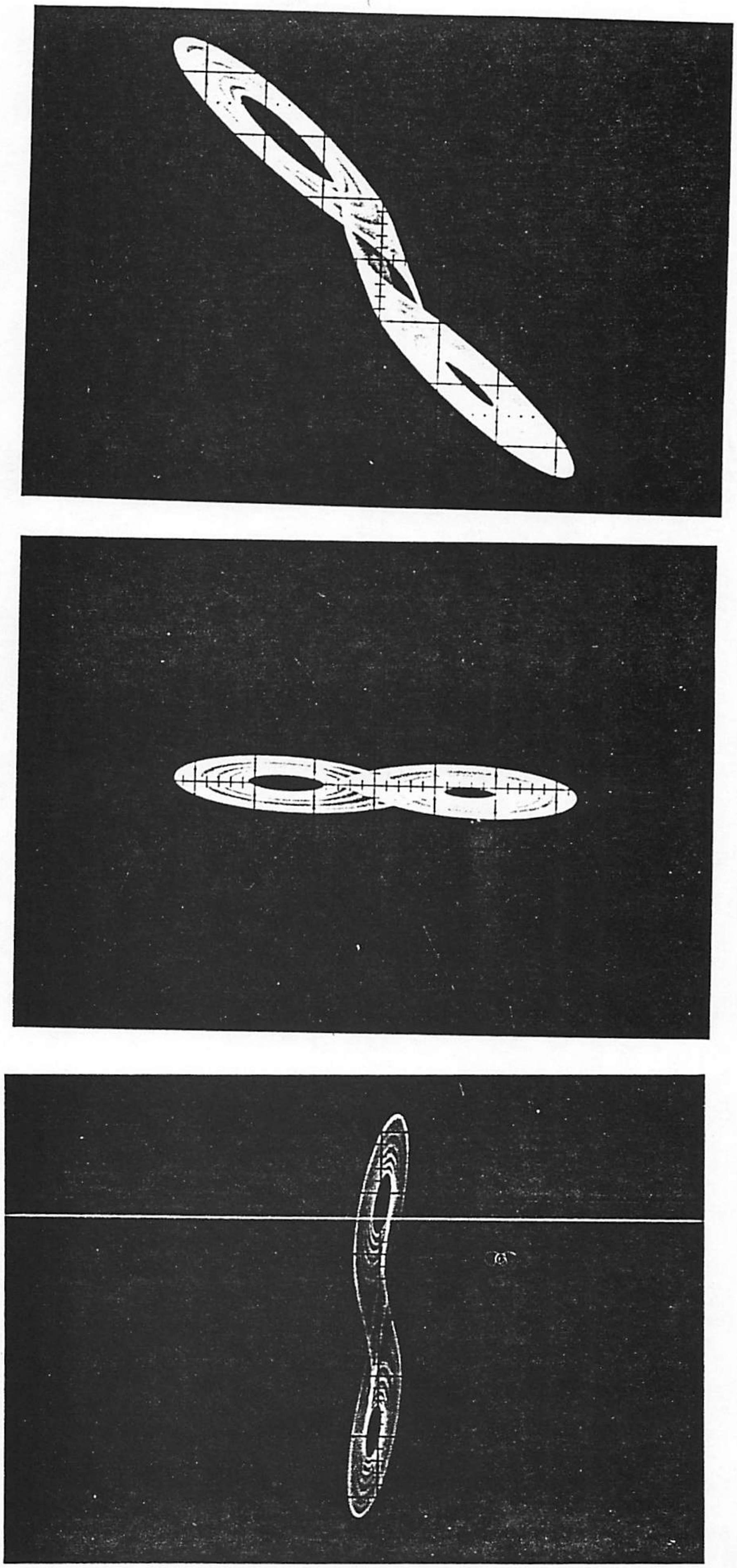

(a)

(b)

(c)

Fig. 3

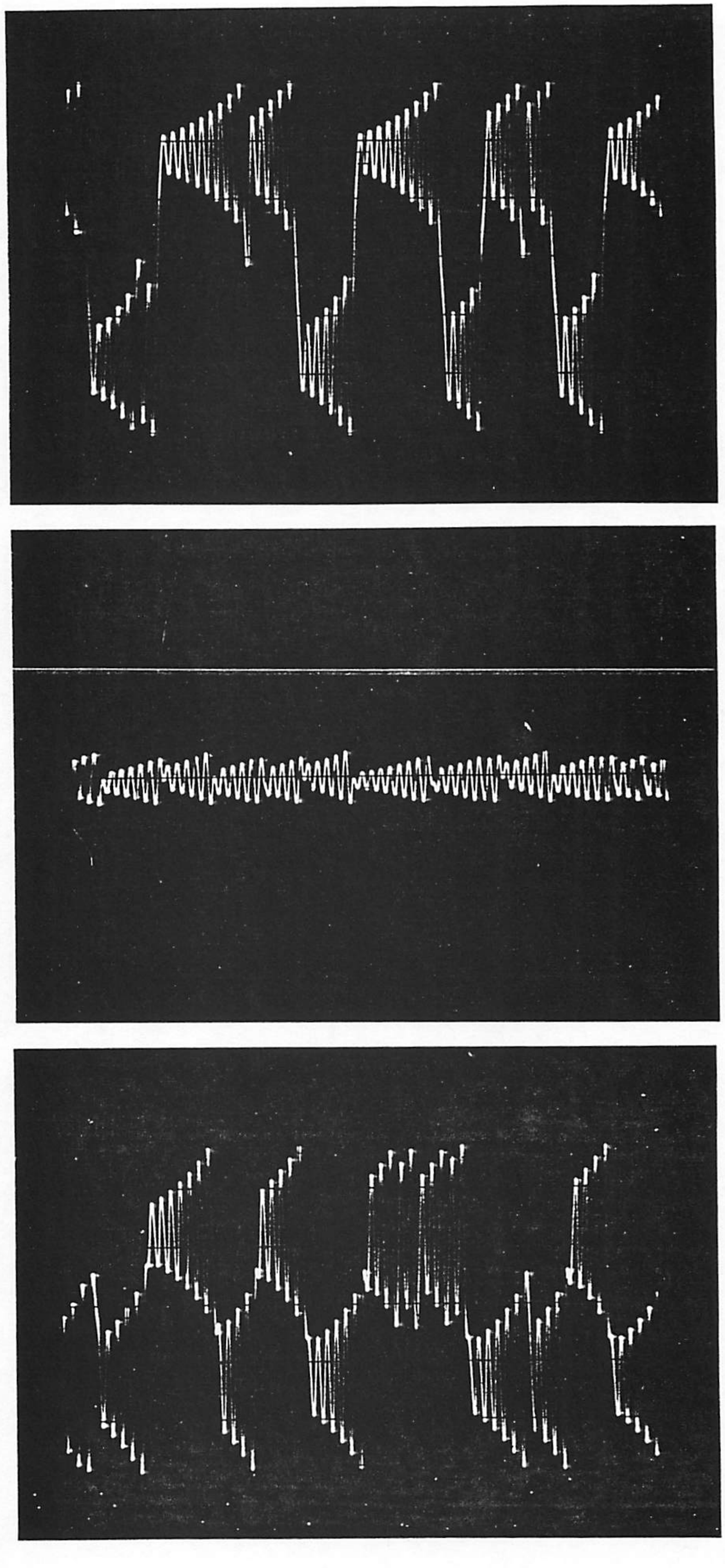

(a)

(b)

(c)

Fig. 4

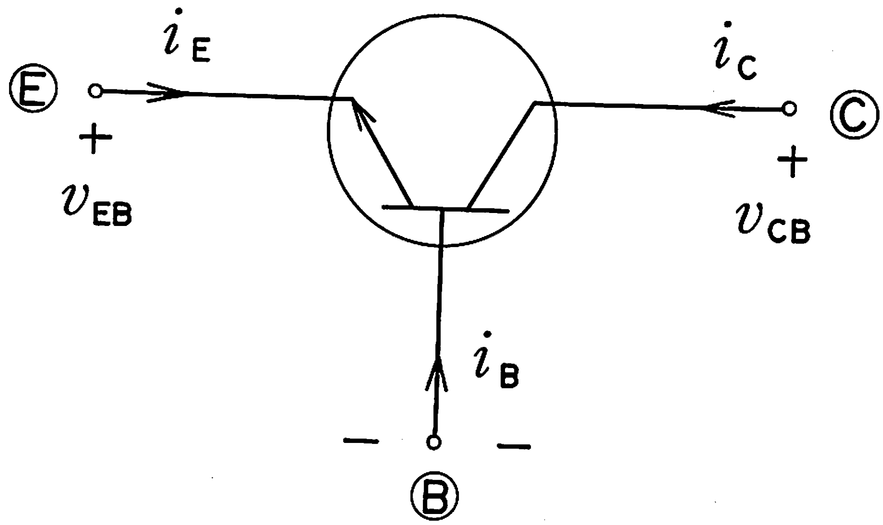

Fig.5

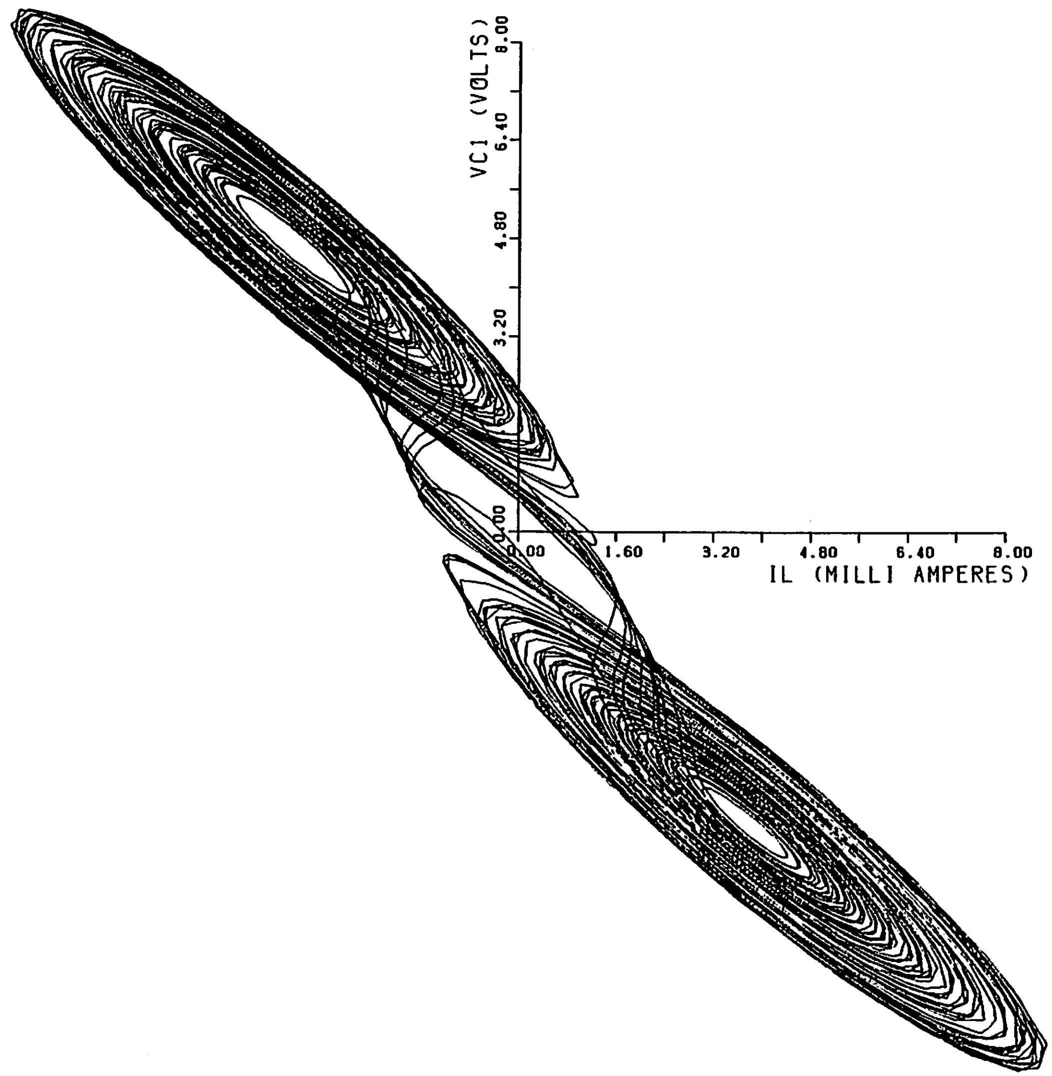
VC1 (VOLTS)
8.00
6.40
4.80
3.20
0.00
0.00
1.60
3.20
4.80
6.40
8.00
IL (MILLI AMPERES)

Fig. 6(a)

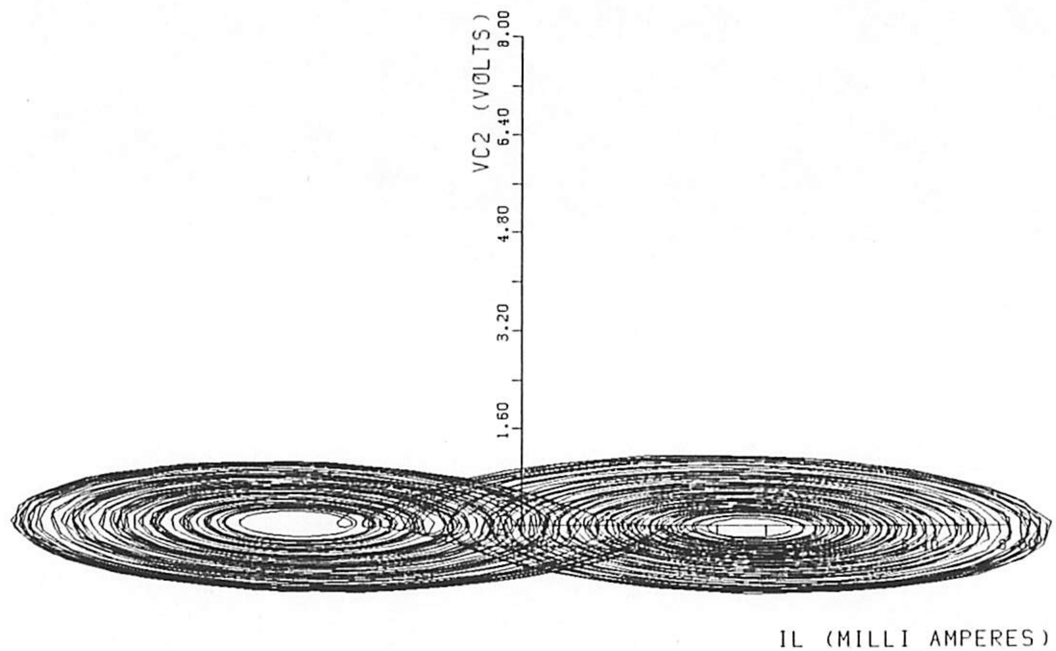

Fig. 6(b)

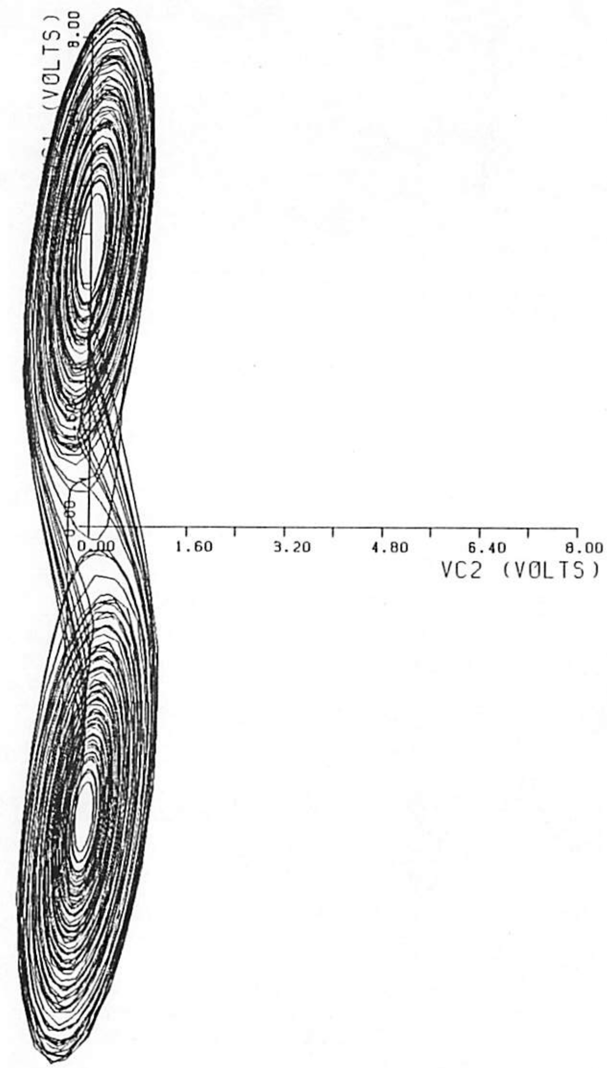

Fig. 6(c)

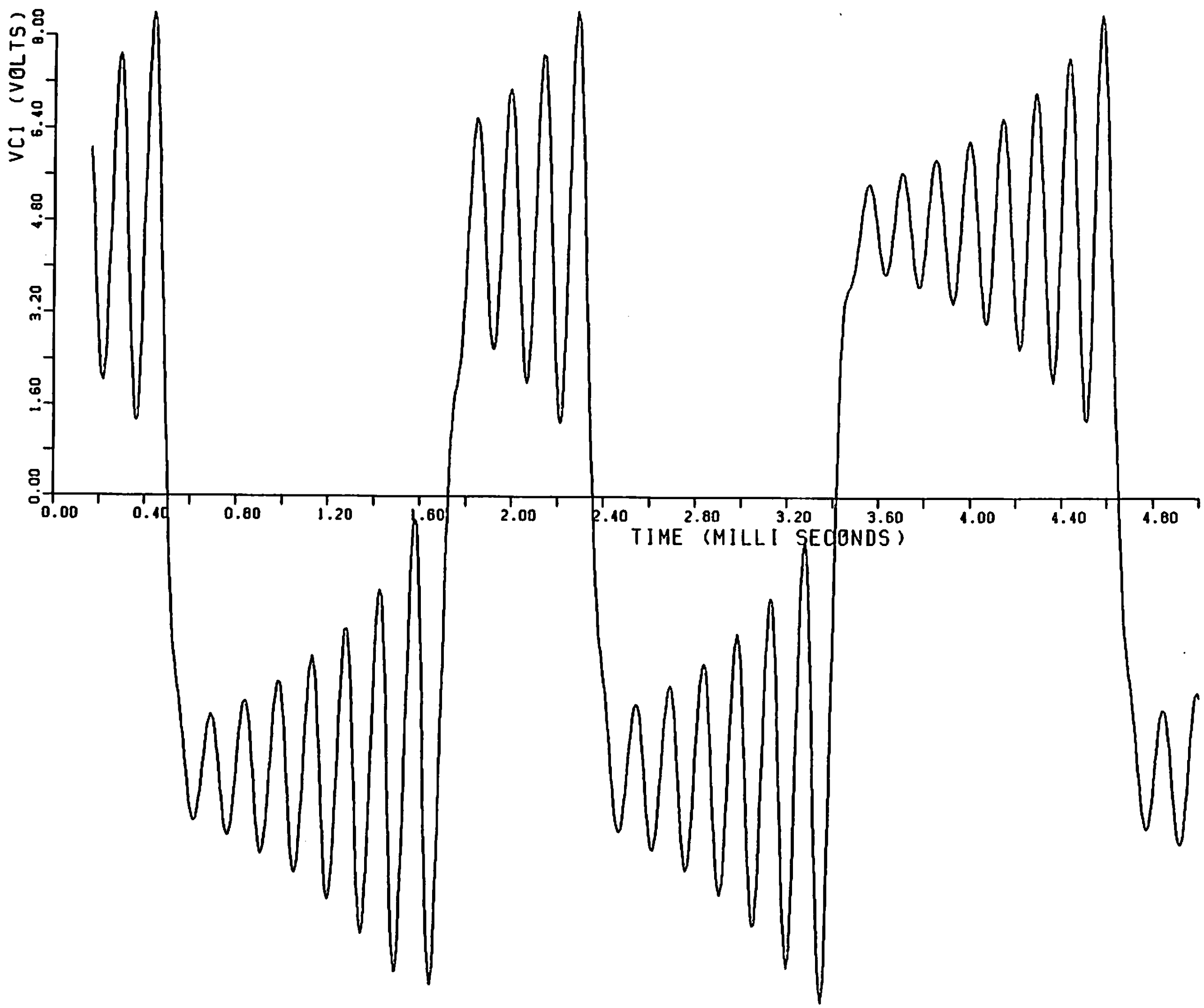
VC1 (VOLTS)
8.00
6.40
4.80
3.20
1.60
0.00
0.00
0.40
0.80
1.20
1.60
2.00
2.40
2.80
3.20
3.60
4.00
4.40
4.80
TIME (MILLI SECONDS)

Fig. 7(a)

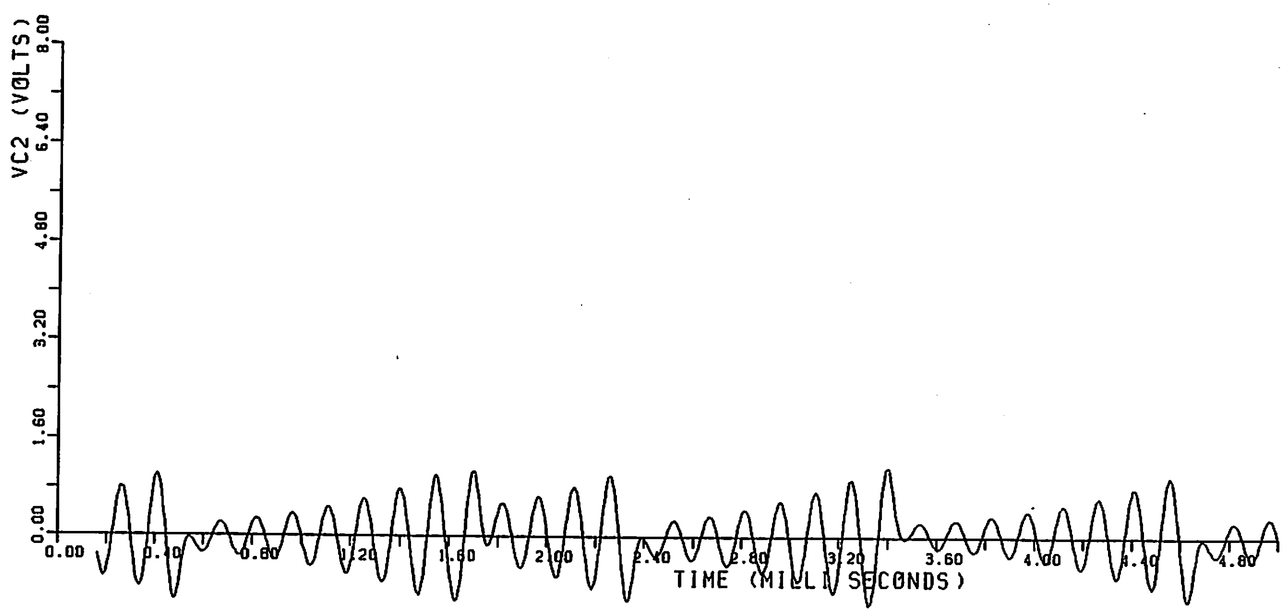
VC2 (VOLTS)
8.00
6.40
4.80
3.20
1.60
0.00
0.00
0.40
0.80
1.20
1.60
2.00
2.40
2.80
3.20
3.60
4.00
4.40
4.80
TIME (MILLI SECONDS)

Fig. 7(b)

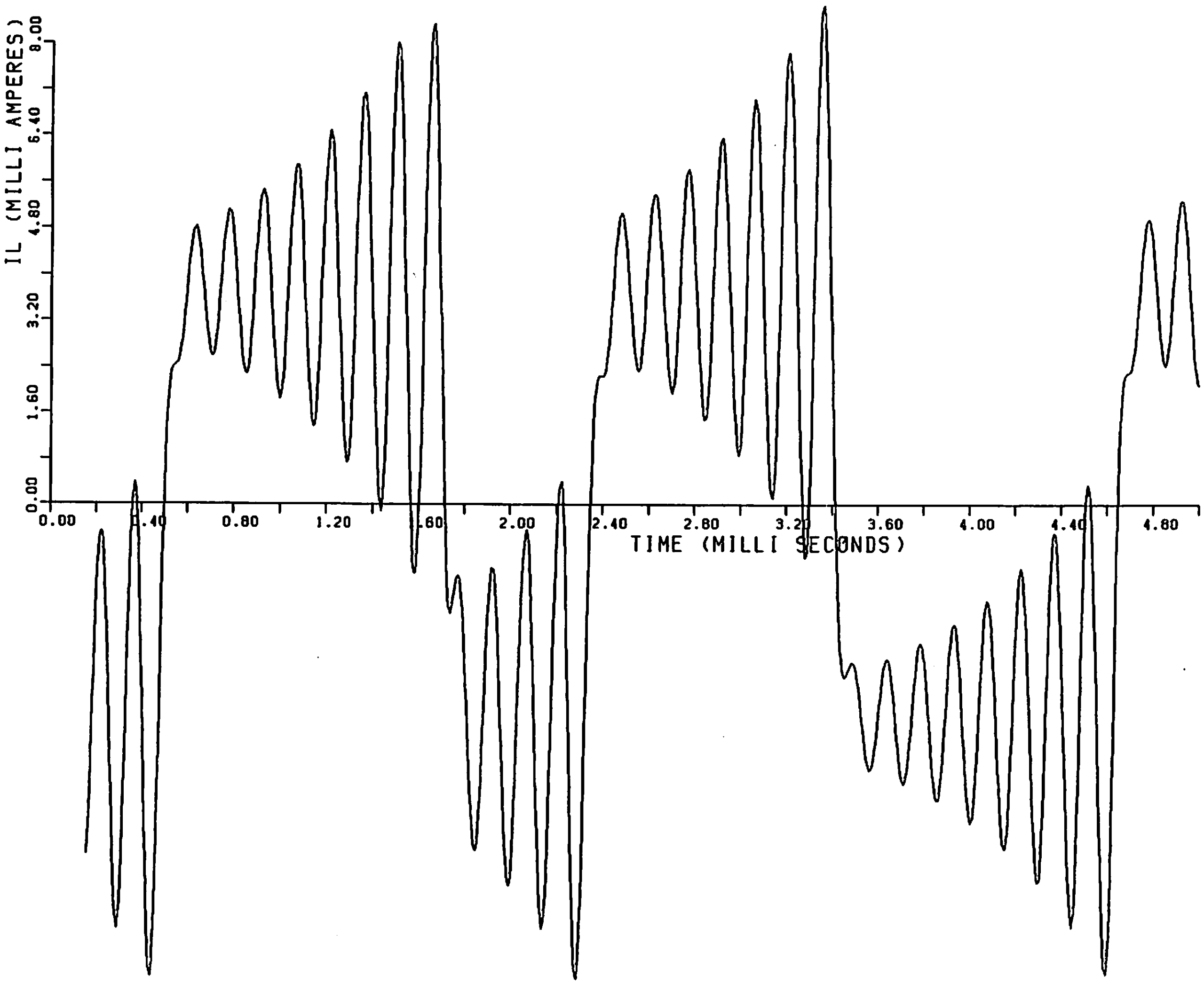
IL (MILLI AMPERES)
0.00
1.60
3.20
4.80
6.40
8.00
0.00
0.40
0.80
1.20
1.60
2.00
2.40
2.80
3.20
3.60
4.00
4.40
4.80
TIME (MILLI SECONDS)

Fig. 7(c)

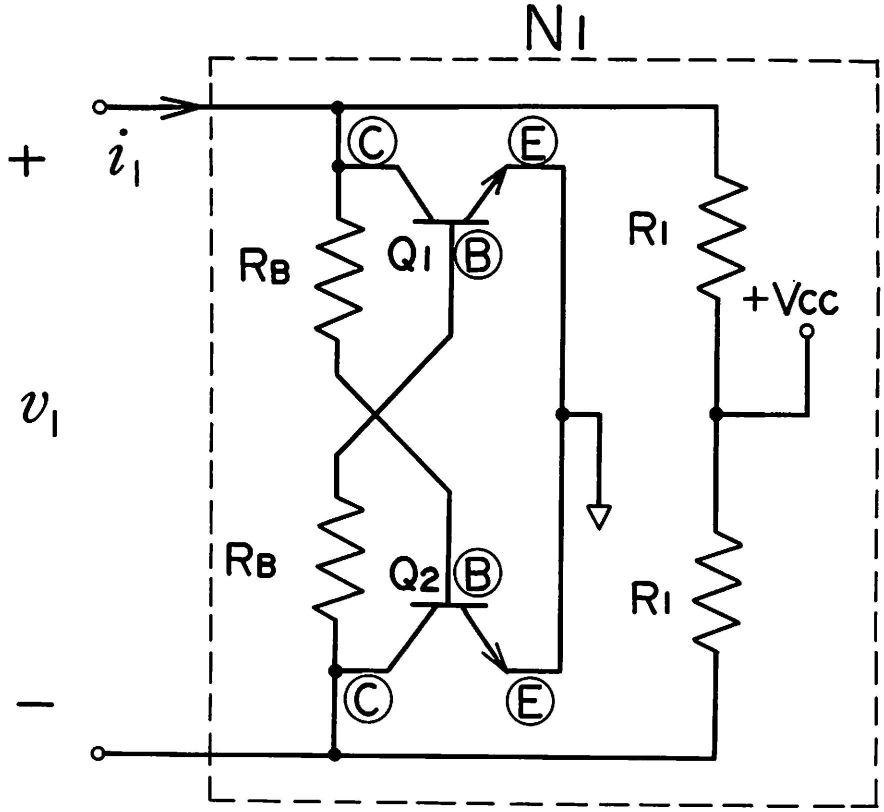

Fig.8

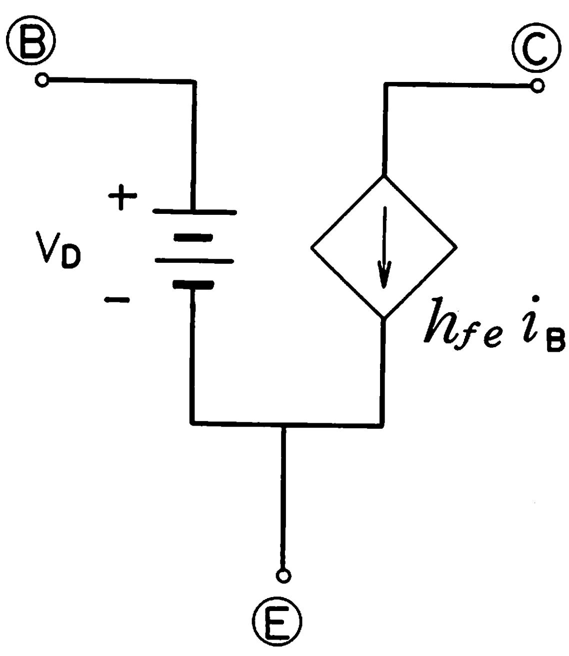

Fig.9

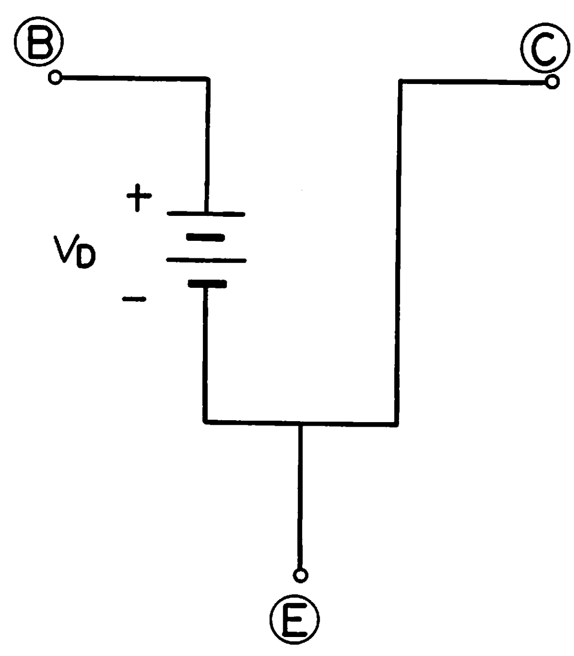

Fig.10

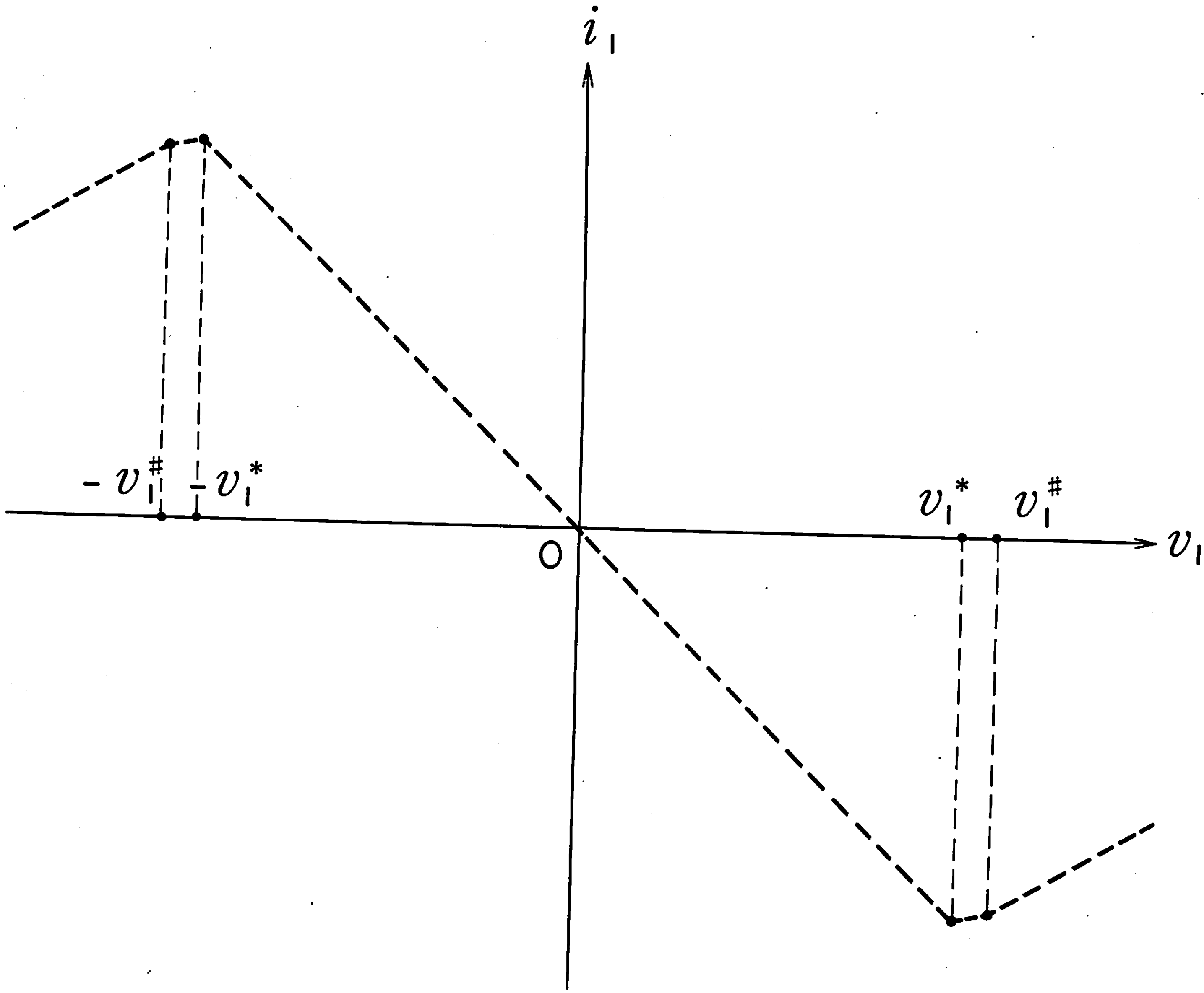

Fig.11

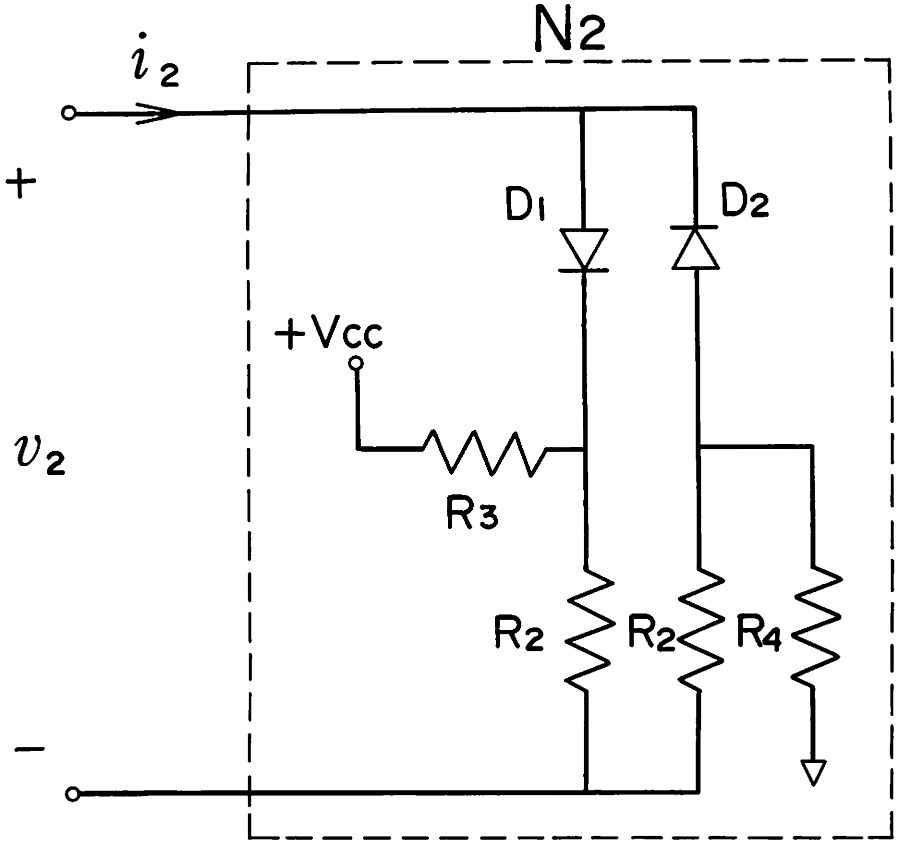

Fig.12

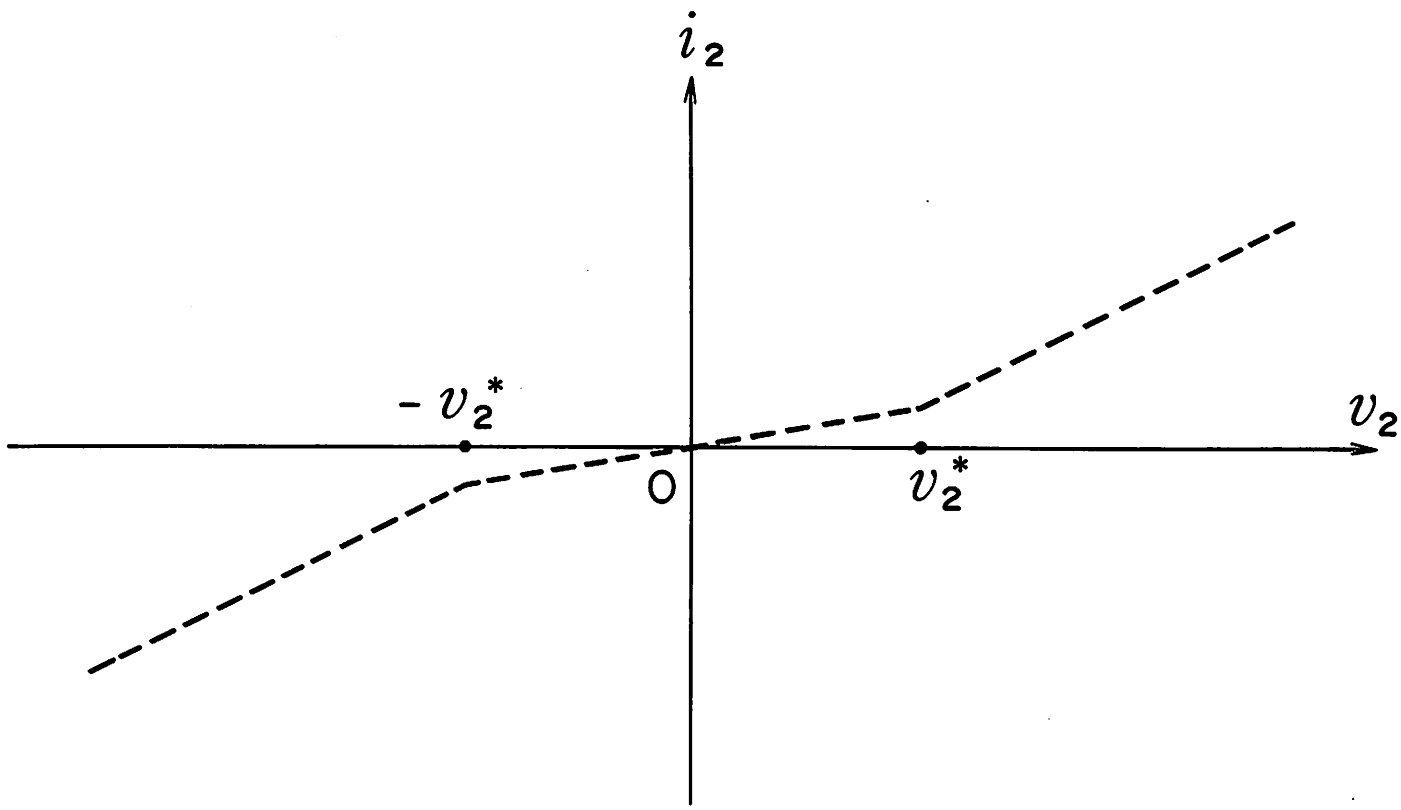

Fig.13

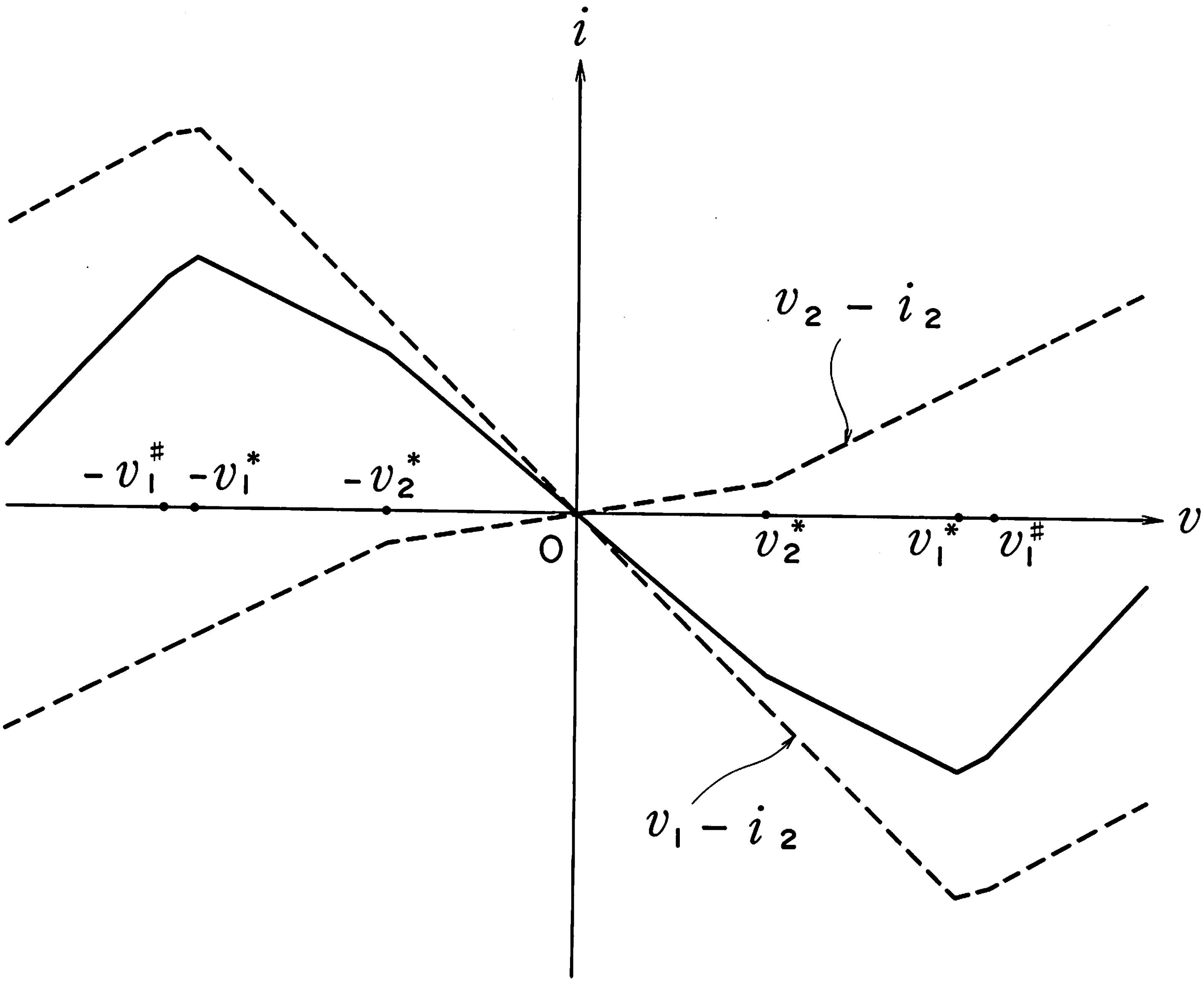

Fig.14